View metadata, citation and similar papers at core.ac.uk

brought to you by CORE

provided by NASA Technical Reports Server

NACA TN 3366

TECH LIBRARY KAFB, NM

0065930

NATIONAL ADVISORY COMMITTEE FOR AERONAUTICS

TECHNICAL NOTE 3366

A METHOD FOR STUDYING THE TRANSIENT BLADE-FLAPPING BEHAVIOR OF LIFTING ROTORS AT EXTREME OPERATING CONDITIONS

By Alfred Gessow and Almer D. Crim

Langley Aeronautical Laboratory
Langley Field, Va.

NACA

Washington
January 1955

AFMDC
TECHNICAL LIBRARY
AFL 2811

TECH LIBRARY KAFB, NM
0065930

NATIONAL ADVISORY COMMITTEE FOR AERONAUTICS

TECHNICAL NOTE 3366

A METHOD FOR STUDYING THE TRANSIENT BLADE-FLAPPING BEHAVIOR OF LIFTING ROTORS AT EXTREME OPERATING CONDITIONS

By Alfred Gessow and Almer D. Crim

SUMMARY

A method is presented for studying the transient behavior of the flapping motion, as well as for calculating the steady-state flapping amplitudes, of free-to-cone and seesaw rotors operating at extreme flight conditions. The method is general and can be applied to blades of any airfoil section, mass distribution, twist, plan-form taper, root cutout, and flapping-hinge geometry. Stall and compressibility effects can also be accounted for.

The method is illustrated by examples of blade-stability calculations of free-to-cone and seesaw rotors at tip-speed ratios equal to or greater than 1.0 and of the transient flapping response of a free-to-cone rotor to arbitrary control inputs at a tip-speed ratio equal to 0.3.

INTRODUCTION

The flapping motion of autogiro and helicopter rotor blades has shown itself, both in theory and actual practice, to be very stable for conventional tip-speed ratios (that is, below about 0.5). Some doubt exists, however, as to the stability of blade motion at tip-speed ratios equal to or greater than 1.0, a question that is of interest in connection with the "unloaded rotor" type of helicopter operation. At these extreme tip-speed ratios, the aerodynamic and blade-inflexibility assumptions employed in existing analyses of the problem (in refs. 1 to 5, for example) become questionable. The aerodynamic factors introducing the most uncertainties in these analyses are the assumptions of unstalled blade sections and incompressible flow, the neglect of the reversed-velocity region, and the use of small-angle assumptions in connection with the section inflow and blade flapping angles.

It is the object of this paper to develop equations and to present a method for determining the stability of blade flapping motion which avoids the no-stall and incompressibility assumptions, as well as some other restrictive aerodynamic assumptions that are normally employed in rotor analyses, and which properly accounts for the reversed-velocity region. The method, which is applicable to numerical solution by automatic computing machines, can also be used to account for the effects of stall, compressibility, and high rotor angle-of-attack operation on the steady-state flapping motion at more conventional helicopter tip-speed ratios and to compute the transient blade-flapping response arising from arbitrary control inputs. No specific terms are included in the equations, however, to account for blade torsional or bending flexibility. The method is illustrated by examples of blade-stability calculations of free-to-cone and seesaw rotors at tip-speed ratios equal to or greater than 1.0 and of the transient flapping response of a free-to-cone rotor to arbitrary control inputs at a tip-speed ratio equal to 0.3.

SYMBOLS

A_1, B_1 coefficients of $-\cos\psi$ and $-\sin\psi$, respectively, in expression for θ; therefore, lateral and longitudinal cyclic-pitch angles, respectively, deg

B tip-loss factor (assumed equal to 0.97 herein); blade elements outboard of radius BR are assumed to have profile drag but no lift

c blade section chord, ft

c_{d_o} section profile drag coefficient

c_e equivalent blade chord (on thrust-moment basis), $\int_{r_c}^{BR} cr^3 dr \Big/ \int_{r_c}^{BR} r^3 dr$, ft

c_l section lift coefficient

dD drag force on blade element, lb

dF_C centrifugal force on blade element, lb

dF_I inertia force on blade element, lb

dL lift force on blade element, lb

dT	thrust on blade element, lb
e	offset of center line of flapping hinge from center line of rotor shaft, ft
g	gravitational acceleration, ft/sec^2
I_h	mass moment of inertia of blade about flapping hinge, $\int_e^R m(r - e)^2 dr$, $slug\text{-}ft^2$
m	mass of blade per foot of radius, slugs/ft
M_C	centrifugal-force moment of blade about flapping hinge, lb-ft
M_I	inertia-force moment of blade about flapping hinge, lb-ft
M_T	thrust moment of blade about flapping hinge, lb-ft
M_W	weight moment of blade about flapping hinge, lb-ft
M_W'	weight moment of blade about flapping hinge at zero flapping, $\int_e^R mg(r - e)dr$, lb-ft
p	helicopter rolling velocity, radians/sec
q	helicopter pitching velocity, radians/sec
r	distance measured along blade from axis of rotation to blade element, ft
R	blade radius, ft
t	time, sec
U	resultant velocity perpendicular to blade-span axis at blade element, ft/sec
U_{P_s}	component at blade element of resultant velocity perpendicular both to blade-span axis and U_{T_s}, ft/sec
U_{T_s}	component at blade element of resultant velocity perpendicular to blade-span axis and to shaft axis, ft/sec

$u = U/\Omega R$

$u_{P_s} = U_{P_s}/\Omega R$

$u_{T_s} = U_{T_s}/\Omega R$

v	induced inflow velocity at rotor (positive downward), ft/sec
V	velocity along flight path, ft/sec
x	ratio of blade-element radius to rotor-blade radius, r/R
α_s	angle between shaft axis and plane perpendicular to flight path, positive when axis is pointing rearward, deg
α_r	blade-element angle of attack, measured from line of zero lift, deg
β	blade flapping angle with respect to shaft at particular azimuth position, radians
$\dot{\beta},\ddot{\beta}$	first and second derivatives of β with respect to time t
$\bar{\beta},\bar{\bar{\beta}}$	first and second derivatives of β with respect to azimuth angle ψ
γ'	mass constant of rotor blade, $c_e\rho R^4/I_h$
θ_0	collective-pitch angle at blade root, average value of instantaneous blade-root pitch angle around azimuth, deg
$\theta_{.75}$	collective-pitch angle at 0.75 blade radius, deg
θ_1	difference between root and tip pitch angles, positive when tip angle is larger, deg
Θ	instantaneous blade-section pitch angle; angle between line of zero lift of blade section and plane perpendicular to rotor shaft, $\theta_0 + \theta_1 x - A_1 \cos\psi - B_1 \sin\psi$, deg
λ_s	inflow ratio, $\dfrac{V \sin\alpha_s - v}{\Omega R}$
μ_s	tip-speed ratio, $\dfrac{V \cos\alpha_s}{\Omega R}$

$\xi = e/R$

ρ mass density of air, slugs/cu ft

ϕ inflow angle at blade element in plane perpendicular to blade-span axis, $\tan^{-1} U_{P_S}/U_{T_S}$, deg

ψ blade azimuth angle measured from downwind position in direction of rotation, deg

Ω rotor angular velocity, radians/sec

Subscript:

c radius of cutout, that is, radius at which lifting surface of blade begins

METHOD OF ANALYSIS

Reference-Axis System

In the analysis for the free-to-cone rotor as developed herein, the flapping hinge may be offset radially from the center line of the shaft. For such a configuration, flapping and feathering motions are not directly equivalent, and all angles and velocities are therefore referred to an axis coinciding with the center line of the rotor shaft. Also, even for zero hinge offset, the shaft axis is a convenient reference axis for cases in which the effect of arbitrary cyclic- or collective-pitch input on the blade transient motion is being studied. The rotor shaft is therefore used as the reference axis in this paper, although it sometimes may be more convenient to use the no-feathering axis as the reference, inasmuch as it is independent of fuselage moment characteristics and center-of-gravity location.

Derivation of Blade-Flapping Equations

The differential equation of blade flapping motion is derived for a free-to-cone rotor by equating the blade aerodynamic and mass moments about the flapping hinge. The origin of the various moments is shown in figure 1(a), and the resulting equation is

$$M_T - M_C - M_I - M_W = 0 \qquad (1)$$

Expressions for the moments will now be derived. The centrifugal-force moment is

$$M_C = \int_e^R m\Omega^2(r - e)\Big[e + (r - e)\cos\beta\Big]\sin\beta\, dr \tag{2}$$

but

$$\int_e^R m(r - e)^2\, dr = I_h \tag{3}$$

and

$$\int_e^R mg(r - e)\cos\beta\, dr = M_W = M_W'\cos\beta \tag{4}$$

(It should be noted that, because M_W is small in relation to the other blade moments, the cosine effect of a shaft tilt on M_W has been neglected.) After equations (3) and (4) are substituted into equation (2), the expression for centrifugal-force moment becomes

$$M_C = \Omega^2\sin\beta\Big(I_h\cos\beta + \frac{e}{g}M_W'\Big) \tag{5}$$

The expression for blade inertia moment is

$$M_I = \int_e^R m\ddot{\beta}(r - e)^2 dr$$

$$= \ddot{\beta}I_h \tag{6}$$

The independent variable can be changed from t to ψ as follows:

$$\left.\begin{aligned}\dot{\beta} &= \Omega\frac{d\beta}{d\psi} = \Omega\beta' \\ \ddot{\beta} &= \Omega\frac{d^2\beta}{d\psi\, dt} = \Omega^2\frac{d^2\beta}{d\psi^2} = \Omega^2\beta''\end{aligned}\right\} \tag{7}$$

and equation (6) becomes

$$M_I = I_h \Omega^2 \ddot{\beta} \tag{8}$$

The expression for thrust moment may be written with the aid of figure 1 as

$$M_T = \int_{r_c}^{BR} \frac{1}{2}\rho U^2 c(r - e)c_l \cos \phi \, dr + \int_{r_c}^{R} \frac{1}{2}\rho U^2 c(r - e)c_{d_o} \sin \phi \, dr \tag{9}$$

The profile-drag contribution to the thrust becomes significant primarily in the reversed-velocity region at flight conditions involving high inflow angles and high tip-speed ratios. It is assumed, of course, that the cut-out r_c is equal to or larger than the offset e, so that no moment is computed for that part of the blade inboard of the flapping hinge. Let

$$\left.\begin{aligned} x &= \frac{r}{R} \\ \xi &= \frac{e}{R} \\ u &= \frac{U}{\Omega R} \end{aligned}\right\} \tag{10}$$

Substituting equations (10) into equation (9) yields

$$M_T = \frac{1}{2}\rho c \Omega^2 R^4 \left[\int_{x_c}^{B} u^2(x - \xi)c_l \cos \phi \, dx + \int_{x_c}^{1.0} u^2(x - \xi)c_{d_o} \sin \phi \, dx \right] \tag{11}$$

The section nondimensional resultant velocity u and the inflow angle ϕ may be found from the following equations:

$$u = \left(u_{P_s}^2 + u_{T_s}^2\right)^{1/2} \tag{12}$$

$$u_{P_s} = \lambda_s \cos \beta - (x - \xi)\dot{\bar{\beta}} - \mu_s \sin \beta \cos \psi + \frac{q}{\Omega} x \cos \psi + \frac{p}{\Omega} x \sin \psi \tag{13}$$

$$u_{T_s} = \xi + (x - \xi) \cos \beta + \mu_s \sin \psi \tag{14}$$

$$\phi = \tan^{-1} \frac{U_{P_s}}{U_{T_s}} \tag{15}$$

(Note that, for the sake of simplicity, for terms involving pitching and rolling velocities in eq. (13) the helicopter is assumed to pitch and roll about the rotor hub.)

The section lift coefficient c_l and drag coefficient c_{d_o} can be found from appropriate airfoil data. It should be noted that the method does not require an analytical representation of the section lift and drag characteristics. Thus, the airfoil characteristics corresponding to the particular blade section and surface condition can be used, and stall, Mach number, and Reynolds number effects can be accounted for whenever they are deemed significant.

The section angle of attack can be found from the following relation:

$$\alpha_r = \Theta + \phi$$

$$= \theta_0 + \theta_1 x - A_1 \cos \psi - B_1 \sin \psi + \phi \tag{16}$$

In this equation all the angles are in degrees.

Substituting equations (4), (5), (8), and (11) into equation (1) and dividing through by $I_h\Omega^2$ yields

$$\frac{1}{2}\frac{\rho c R^4}{I_h}\left[\int_{x_c}^{B} u^2(x-\xi)c_l \cos\phi\, dx + \int_{x_c}^{1.0} u^2(x-\xi)c_{d_o} \sin\phi\, dx\right] -$$

$$\sin\beta\left(\cos\beta + \frac{eM_W'}{gI_h}\right) - \ddot{\beta} - \frac{M_W'\cos\beta}{\Omega^2 I_h} = 0 \tag{17}$$

By definition,

$$\gamma' = \frac{\rho c R^4}{I_h} \tag{18}$$

and equation (17) becomes

$$\frac{1}{2}\gamma'\left[\int_{x_c}^{B} u^2(x-\xi)c_l \cos\phi\, dx + \int_{x_c}^{1.0} u^2(x-\xi)c_{d_o} \sin\phi\, dx\right] -$$

$$\sin\beta\left(\cos\beta + \frac{eM_W'}{gI_h}\right) - \ddot{\beta} - \frac{M_W'\cos\beta}{\Omega^2 I_h} = 0 \tag{19}$$

If β is considered to be a small angle (that is, less than 20°), as it usually is, the equations can be somewhat simplified in that $\cos\beta$ can be assumed to be equal to 1.0. It will also be noted that, although a uniform-chord blade was assumed in the development of the thrust-moment equation, in numerical work blades of any plan form can be handled just as simply by allowing c to remain beneath the integral sign. The blade mass constant γ', which is of value for blade-motion comparisons between

blades of different design, may then be retained by basing γ' on an equivalent chord c_e equal to $\int_{r_c}^{BR} cr^3 dr \Big/ \int_{r_c}^{BR} r^3 dr$.

Equation (19) is the basic differential equation describing the flapping motion of a free-to-cone rotor. As written, the aerodynamic part of the equation is very general in that it can handle blades of any airfoil section, mass distribution, twist, plan-form taper, root cutout, and flapping-hinge offset and can account for the effects of helicopter pitching or rolling velocities. The effect of flapping-hinge geometry where blade flapping or lagging motions result in pitch-angle changes can be simply considered by the addition of the appropriate terms in equation (16). Stall and compressibility effects can be accounted for to the extent of using actual airfoil section data that correspond to the entire range of angle of attack and Mach number encountered at all points of the disk, including the reversed-velocity region. (The section Mach number is simply computed as $u\Omega R$ divided by the speed of sound.) No small-angle limitations have been made regarding the blade inflow and flapping angles, although it is assumed in the analysis that the blades are rigid in torsion and in bending and that radial flow effects can be neglected. The assumption is also made that the rotational speed is a constant. Such an assumption is considered to be reasonable in that some form of rotor-speed control will probably be incorporated in most unloaded-rotor configurations because of the extreme sensitivity of rotor speed to angle-of-attack changes at those conditions.

The differential equation of blade motion for the seesaw rotor may be derived in an analogous manner, the only difference being that the moments of each blade about the seesaw hinge are equated. The resulting equation is

$$\frac{1}{2}\gamma'\left[\left(\int_{x_c}^{B} u^2 x c_l \cos\phi\, dx + \int_{x_c}^{1.0} u^2 x c_{d_o} \sin\phi\, dx\right)_{\psi} - \left(\int_{x_c}^{B} u^2 x c_l \cos\phi\, dx + \int_{x_c}^{1.0} u^2 x c_{d_o} \sin\phi\, dx\right)_{\psi+\pi}\right] - \left(2\sin\beta\cos\beta - 2\bar{\bar{\beta}}\right)_{\psi} = 0 \tag{20}$$

where ψ and $\psi + \pi$ indicate the instantaneous azimuth positions of the two blades. It should be remembered that, in evaluating equation (13) for the seesaw rotor, the signs of β and $\bar{\beta}$ for each blade are opposite. Thus, considering one blade at a particular azimuth position ψ,

$$u_{P_s} = \lambda_s \cos \beta - (x - \xi)\bar{\beta} - \mu_s \sin \beta \cos \psi + \frac{q}{\Omega} x \cos \psi + \frac{p}{\Omega} x \sin \psi$$

and, for the opposite blade at $\psi + \pi$,

$$u_{P_s} = \lambda_s \cos \beta + (x - \xi)\bar{\beta} + \mu_s \sin \beta \cos \psi + \frac{q}{\Omega} x \cos \psi + \frac{p}{\Omega} x \sin \psi$$

Solution of Blade-Flapping Equations

Blade-flapping amplitude and stability may be studied by solving differential equation (19) or (20) for the flapping amplitude β as a function of azimuth angle ψ. Because the equations are nonhomogeneous and nonlinear with varying coefficients that contain integral expressions which become very complex when such items as stall and compressibility are being considered, an explicit solution is not feasible and numerical step-by-step methods must be used.

The suggested procedure for solving equation (19) or (20) may be outlined as follows:

(1) At some convenient azimuth position, assume arbitrary initial values of $\beta = \bar{\beta} = 0$.

(2) Compute the thrust moment at this selected azimuth position by evaluating the thrust-moment integral at several radial stations and integrating the results by numerical or graphical means.

(3) Solve the resulting equation for $\bar{\bar{\beta}}$.

(4) Repeat the above steps at the next succeeding azimuth position using values of β and $\bar{\beta}$ obtained by integrating the quantity $\bar{\bar{\beta}}$. The Runge-Kutta method described in reference 6 is suitable for this phase of the problem.

(5) Continue this process at successive azimuth positions until β either reaches a steady-state value (that is, repeats itself periodically) for a stable condition or diverges for an unstable one.

Some saving in computing time is possible, particularly when steady-state values are being computed, by using estimated values of β and $\bar{\beta}$ in step (1) rather than assuming them equal to zero.

Physically, the blade response as calculated by this method may be visualized either as that resulting from the transition of the rotor blade from an arbitrary out-of-trim position to one of equilibrium (for a stable case) or, alternatively, the motion resulting from the sudden release of a blade that has been restrained from flapping.

The method is also applicable to computing the transient response of blade flapping due to arbitrary control displacements (by merely inserting any desired cyclic- or collective-pitch control sequence into eq. (16) at some time after steady-state conditions have been attained). In addition, the method may be used to determine steady-state flapping values at flight conditions outside the scope of conventional rotor theory.

APPLICATIONS

In order to illustrate some applications of the method that are of current interest, the flapping stability of a number of unloaded-rotor configurations operating at extreme tip-speed ratios, as well as the transient flapping motion occurring during a high-speed pull-up maneuver of a conventional helicopter, was investigated. Most of the cases that were studied involved the free-to-cone rotor, but two seesaw-rotor examples are included for comparison in the unloaded-rotor application. Aside from type of rotor, the primary variables considered are the tip-speed ratio μ_s and the blade mass constant γ'.

Calculation Procedure

The blade-flapping equations were evaluated by the Runge-Kutta method. Azimuth intervals of 20° were used, except where noted. (Although the Runge-Kutta method entails calculations at intermediate stations and is thus more lengthy than some other numerical methods that were tried, it was found to be more accurate.) The thrust-moment contribution at six radial stations was evaluated in determining the thrust-moment integrals in equations (19) and (20). The calculations were performed at the Langley Laboratory by the Bell Telephone Laboratories X-66744 relay computer, and approximately 50 minutes was required for the calculations at each azimuth position for the free-to-cone rotor. In terms of the more

widely used IBM Card Programmed Electronic Calculator (with a floating decimal board), the estimated time per station would be reduced to 20 minutes. With one of the higher speed machines, such as the Remington Rand Universal Automatic Computer (UNIVAC) or the IBM type 701 electronic data processing machine, the machine time per station would probably be reduced to somewhat less than 1 minute. The seesaw-rotor calculations require about twice the time as those for the free-to-cone rotor.

The section lift and drag curves used in the calculations are shown in figure 2 and are plotted for an angle-of-attack range from 0° to 360°. This method of handling the angles of attack is particularly convenient for automatic-machine computation in that the reversed-velocity region is handled in the same manner as the rest of the disk and thus the use of special instructions is avoided. In order to make the calculated section angle of attack positive over a 360° range, 360° should be added to α_r whenever α_r, as calculated by equation (16), is negative. Thus, for example, a negative angle of attack of -30°, such as might occur in the reversed-velocity region, would, by adding 360°, be expressed as 330°. Values of c_l and c_{d_0} below the stall are represented in figure 2 by the customary linear lift curve and three-term drag polar, whereas values above the stall are approximately in accord with wind-tunnel tests of airfoils through 180° angle of attack (ref. 7). Compressibility effects were not considered in the present examples, although, as previously mentioned, the method of analysis is capable of handling such factors. In addition, the blades had zero hinge offset, were untwisted, and operated with zero cyclic pitch, except where noted.

Flapping-Stability Examples

Free-to-cone rotor.- The calculated blade flapping angles at a flight condition corresponding to an unloaded rotor at $\mu_s = 1.0$ $\left(\theta_{.75} = 0^\circ;\ \lambda_s = 0.038\right)$ are shown in figure 3 for three different mass factors. In each case the flapping motion is stable, in that steady-state values are either reached or approached in a few revolutions, although some initial overshoot of the final value is evident for the lightest blade ($\gamma' = 2.62$). As an indication of the effect of blade mass factor on flapping, the maximum steady-state amplitudes shown in figure 3 are plotted in figure 4 as a function of blade mass factor. The maximum positive flapping amplitude is shown to increase almost linearly with γ'; whereas the maximum negative angle is, for this particular case, almost independent of γ'.

The effect of blade mass constant on the flapping stability and amplitude of a rotor operating at a more extreme flight condition ($\mu_s = 2.2$; $\theta_{.75} = 0^\circ$; $\lambda_s = 0.029$) is shown in figure 5. For ease of representation, the vertical scale is varied for the various values of

γ' in order to account for the larger flapping amplitudes of the lighter blades. The motion is seen to be stable for all the values of γ' represented, although the flapping changes from predominately first harmonic at the lowest values of γ' to a prominent one-half harmonic at the highest values of γ'. The deviation of the dominant frequency of the transient flapping motion from the more normal first-harmonic motion is discussed in reference 2 and may be attributed to the varying spring and damping terms in the blade-flapping equation of motion. The curves in figure 5 show that the heavier blades take a longer time to reach the steady-state condition than the lighter ones do and thus may be considered to be more sluggish in response to a disturbance. Figure 5 also shows that the steady-state flapping amplitudes of the lighter blades appear to be impractically large.

In order to determine the effect of azimuth-interval spacing on the results, the calculations for three values of γ' in figure 5 were carried out in two parts, the first part with 40° increments and the second part with 20° increments. It appears that the larger interval would yield about the same result as the smaller one insofar as the stability of the motion is concerned and that the smaller interval would probably yield a more accurate result for the amplitude of the steady-state motion.

Flapping stability at an even more extreme flight condition ($\mu_s = 3.0$; $\theta_{.75} = 2^\circ$; $\lambda_s = -0.0636$) is investigated in figure 6. The motion is seen to be stable for $\gamma' = 0.10$ and 0.42, although for $\gamma' = 0.42$ the motion includes a one-half-per-revolution harmonic imposed on the basic one-per-revolution frequency. For a lighter set of blades ($\gamma = 2.62$), the motion is purely divergent in less than 1 revolution.

Seesaw rotor.- Computations were made for two seesaw rotors involving different flight conditions and blade mass factors and are shown in figure 7. As in the free-to-cone configuration, the heavier blades show a relatively slow response; whereas the lighter blades show the characteristic initial overshoot. It should be noted that the flight condition corresponding to the light ($\gamma' = 2.62$) seesaw blades in figure 7(a) is identical to that of the light ($\gamma' = 2.62$) free-to-cone blades in figure 6. Although the flapping amplitude of the seesaw blades is large for this condition, it is significant that the motion is stable; whereas the flapping motion of the free-to-cone blades in the identical flight condition is highly divergent. It thus appears that the present method of analysis could be used to indicate likely avenues for improvement.

Transient-Response Example

The calculation of transient response of a rotor blade to arbitrary control inputs under conditions involving extreme rotor stall was carried

out by this method for the case of a free-to-cone rotor operating at a tip-speed ratio equal to 0.3. The helicopter was assumed to be undergoing a pull-up maneuver which involved two arbitrary sequences of longitudinal cyclic- and collective-pitch control movements. For the flight condition chosen, the rotor is only partially stalled inboard before the start of the pull-up and undergoes extensive stall over most of the retreating side of the disk during the maneuver.

The results of the calculation are plotted in figure 8, in which are shown both the blade-motion and control-movement time histories. The steady-state amplitude prior to the control motion was calculated as in the preceding cases. The steady state is very quickly reached (within 2 revolutions) and the amplitude is reasonable. When the cyclic- and collective-pitch controls are moved in accordance with a pull-and-hold procedure, the blade motion responds almost immediately and reaches a new steady-state amplitude that is considerably larger than the amplitude existing before the pull-up. If, instead of a pull-and-hold procedure, the controls are partially returned to their equilibrium position, the maximum positive flapping is reduced, as would be expected, with but little effect on the maximum negative amplitude. It will be noted that the maximum negative amplitude is large and that the method of analysis permits calculations to be made for the study of blade-clearance problems in maneuvers. Similar calculations can be made to investigate the effects of varying the rate and amount of control motion, the phasing between the cyclic- and collective-pitch controls at various flight conditions, and the effect of the pitching or rolling velocity developed during the maneuver.

CONCLUDING REMARKS

A numerical method has been presented for studying the transient flapping behavior as well as for calculating the steady-state blade flapping motion of lifting rotors operating at extreme conditions involving stall and compressibility effects and at very high tip-speed ratios and rotor angles of attack. The method can be applied to free-to-cone and seesaw rotors and to blades of any airfoil section, mass distribution, twist, plan-form taper, root cutout, and flapping-hinge geometry.

The method was applied to the investigation of the effect of tip-speed ratio (equal to or greater than 1.0) and blade mass factor on the flapping stability of unloaded free-to-cone and seesaw rotors and the

effect of a pull-up maneuver on the transient blade response under conditions involving extreme stall at a tip-speed ratio equal to 0.3.

Langley Aeronautical Laboratory,
National Advisory Committee for Aeronautics,
Langley Field, Va., November 3, 1954.

REFERENCES

1. Bennett, J. A. J.: Rotary-Wing Aircraft. V.- Flapping. Aircraft Engineering, vol. XII, no. 135, May 1940, pp. 139-141, 146.

2. Horvay, Gabriel: Rotor Blade Flapping Motion. Quarterly Appl. Math., vol. V, no. 2, July 1947, pp. 149-167.

3. Horvay, Gabriel, and Yuan, S. W.: Stability of Rotor Blade Flapping Motion When the Hinges Are Tilted. Generalization of the "Rectangular Ripple" Method of Solution. Jour. Aero. Sci., vol. 14, no. 10, Oct. 1947, pp. 583-593.

4. Parkus, Henry: The Disturbed Flapping Motion of Helicopter Rotor Blades. Jour. Aero. Sci., vol. 15, no. 2, Feb. 1948, pp. 103-106.

5. Yuan, S. W., and Morduchow, M.: On the Stability of the Transient Motion of Helicopter Blades in Flapping and Lagging. Reissner Anniversary Vol.: Contributions to Applied Mechanics. J. W. Edwards (Ann Arbor, Mich.), 1949, pp. 163-181.

6. Scarborough, James B.: Numerical Mathematical Analysis. Second ed., The John Hopkins Press (Baltimore), 1950, pp. 299-303.

7. Pope, Alan: Summary Report of the Forces and Moments Over an NACA 0015 Airfoil Through 180° Angle of Attack. Aero Digest, vol. 58, no. 4, Apr. 1949, pp. 76-78, 100.

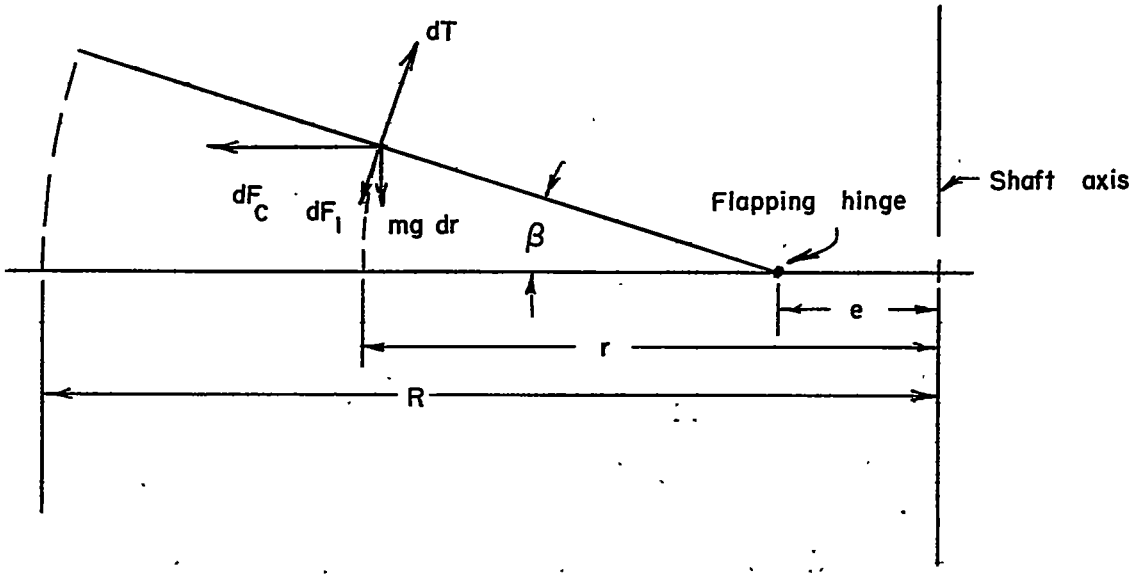

(a) Source of moments about flapping hinge.

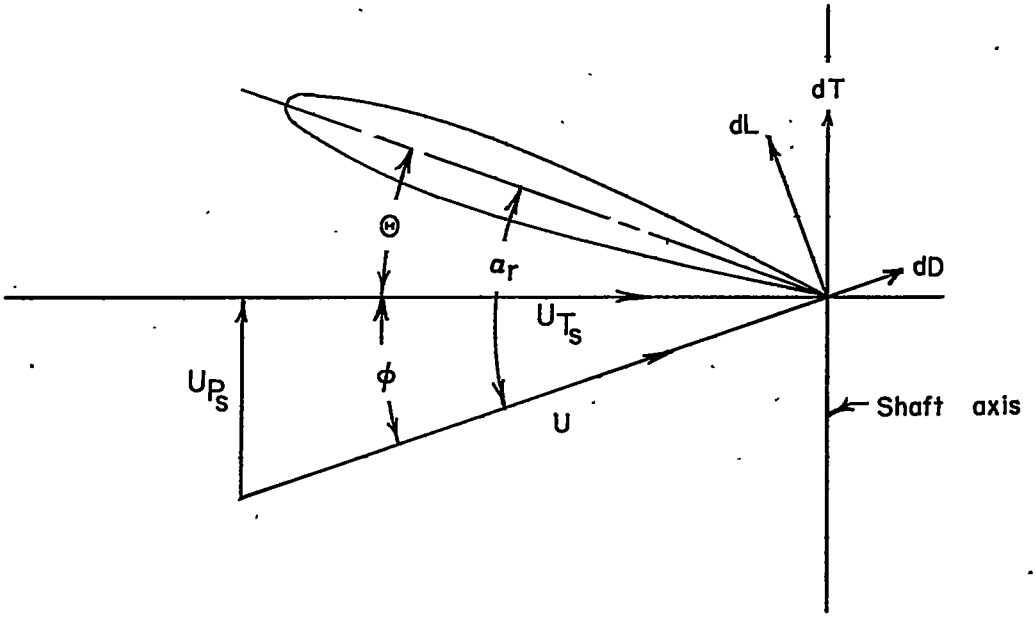

(b) Velocities and angles at blade element.

Figure 1.- Forces and velocities acting at a blade element.

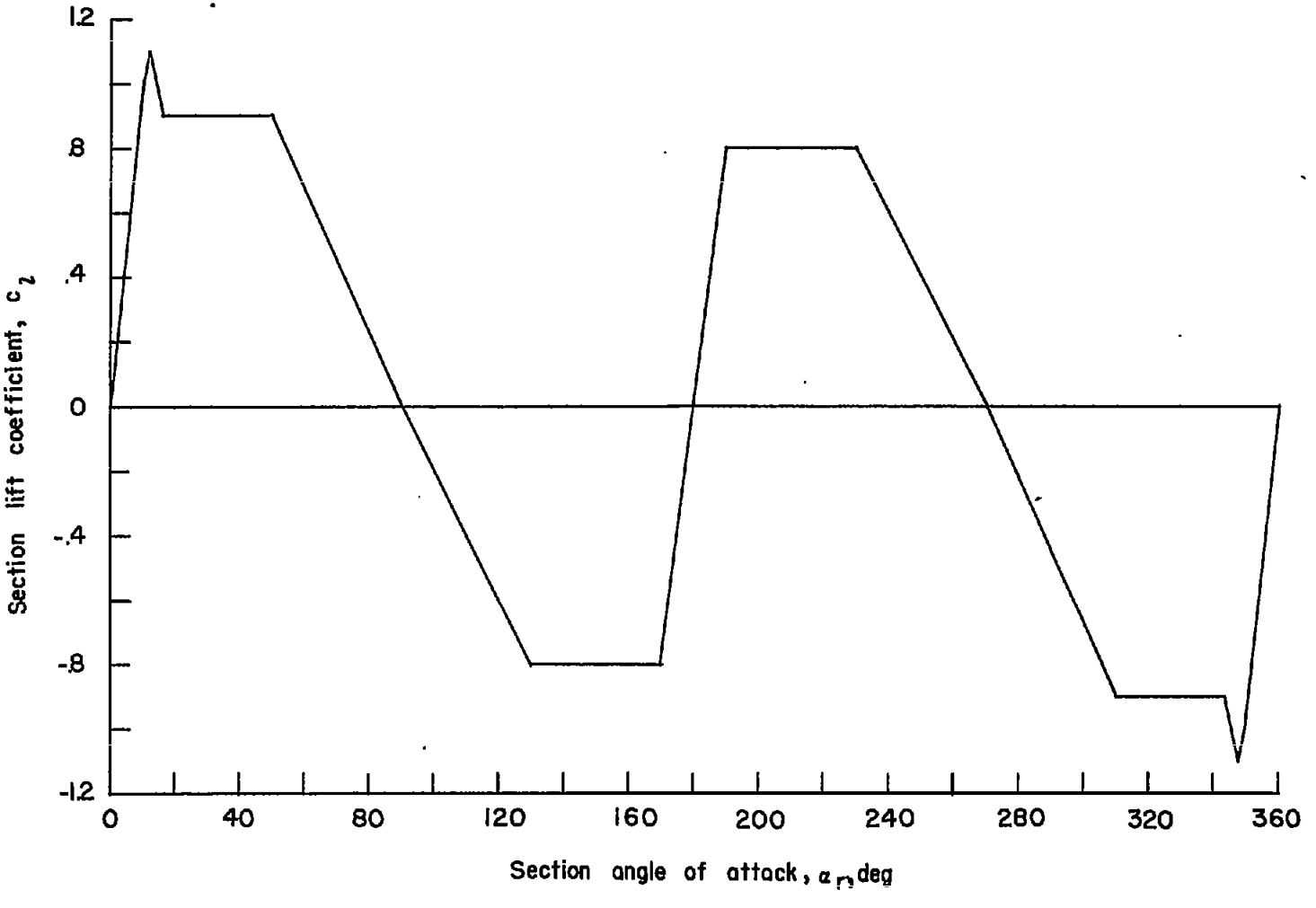

(a) c_l plotted against α_r.

Figure 2.- Lift and drag curves used in illustrative calculations.

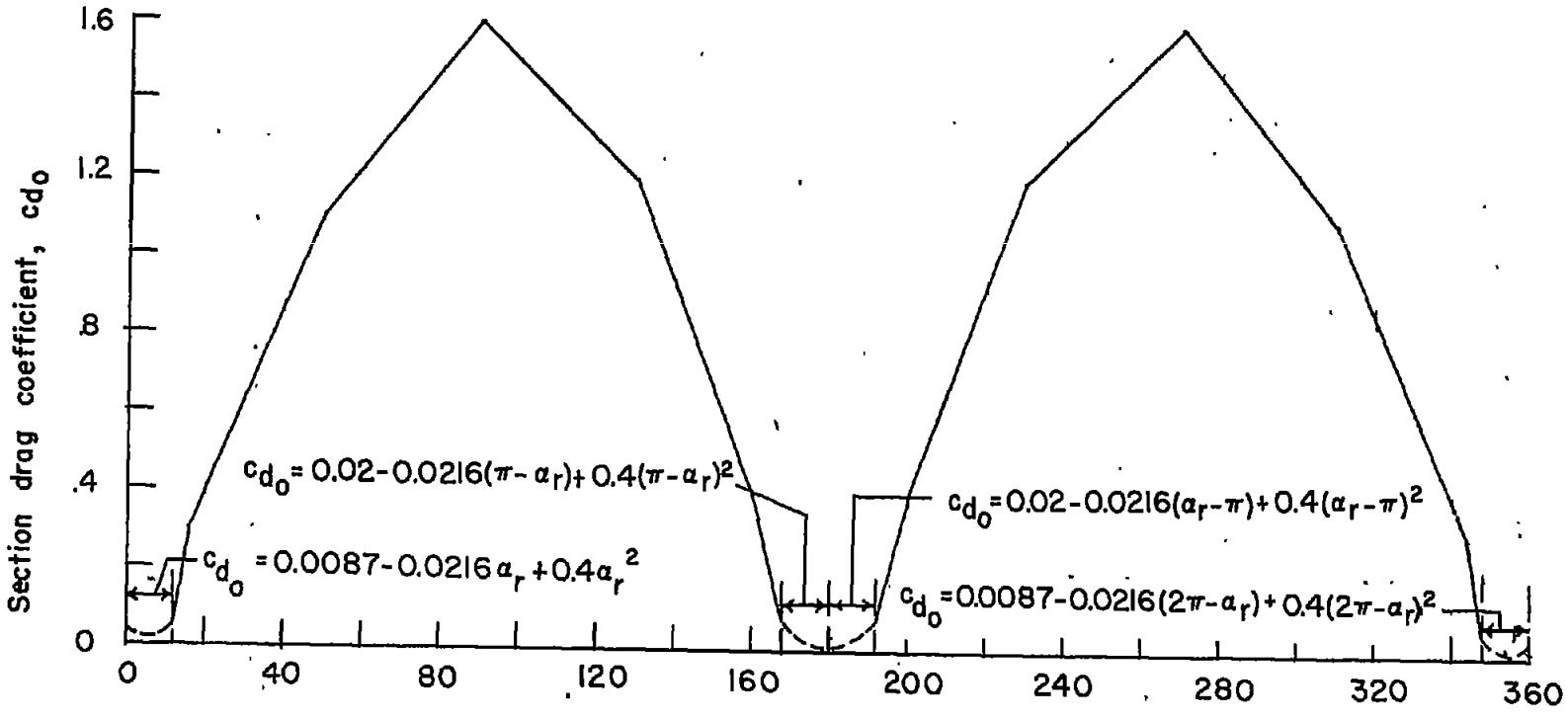

(b) c_{d_o} plotted against α_r.

Figure 2.- Concluded.

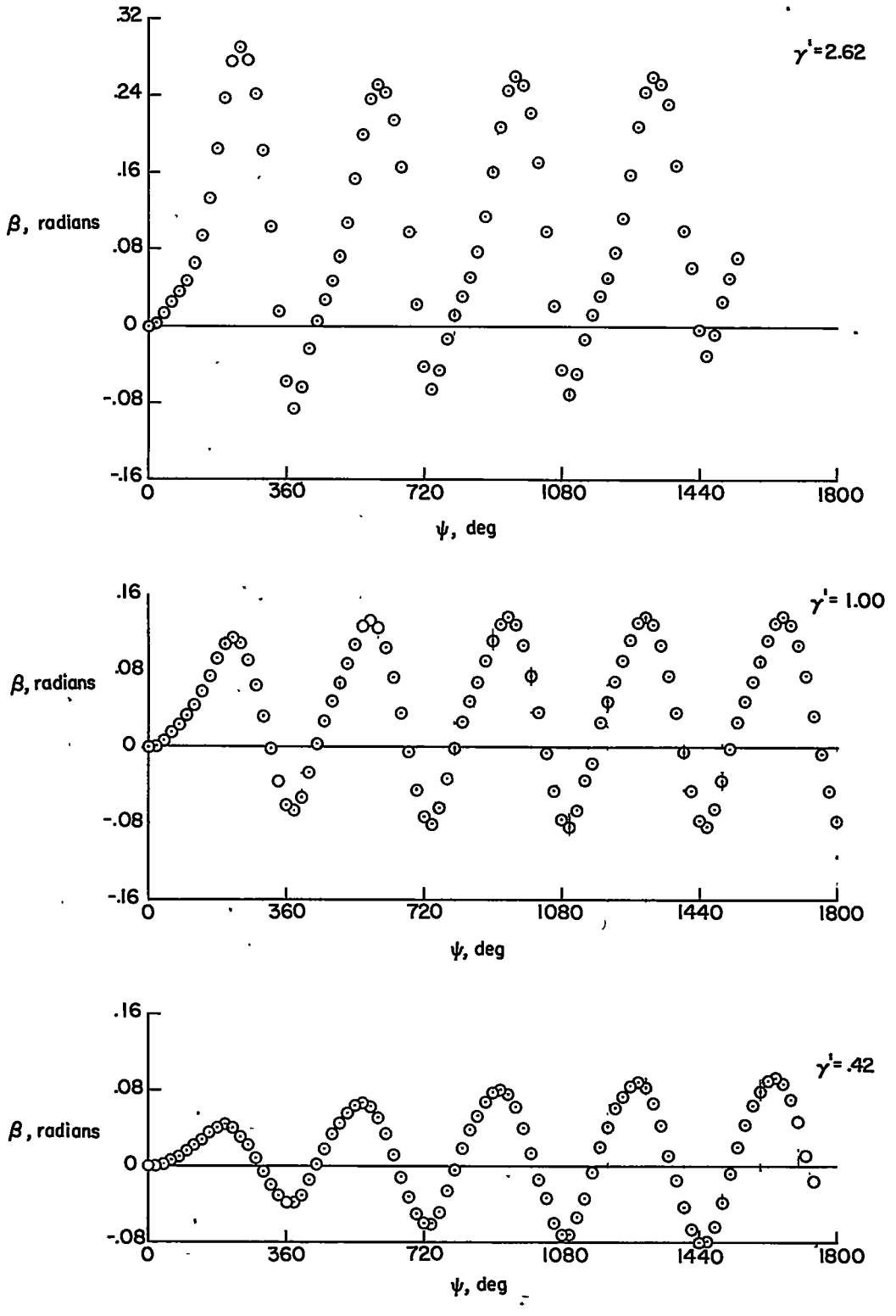

Figure 3.- Calculation of transient blade-flapping motion of free-to-cone rotor at $\mu_s = 1.0$, $\theta_{.75} = 0^\circ$, $\theta_1 = 0^\circ$, and $\lambda_s = 0.038$.

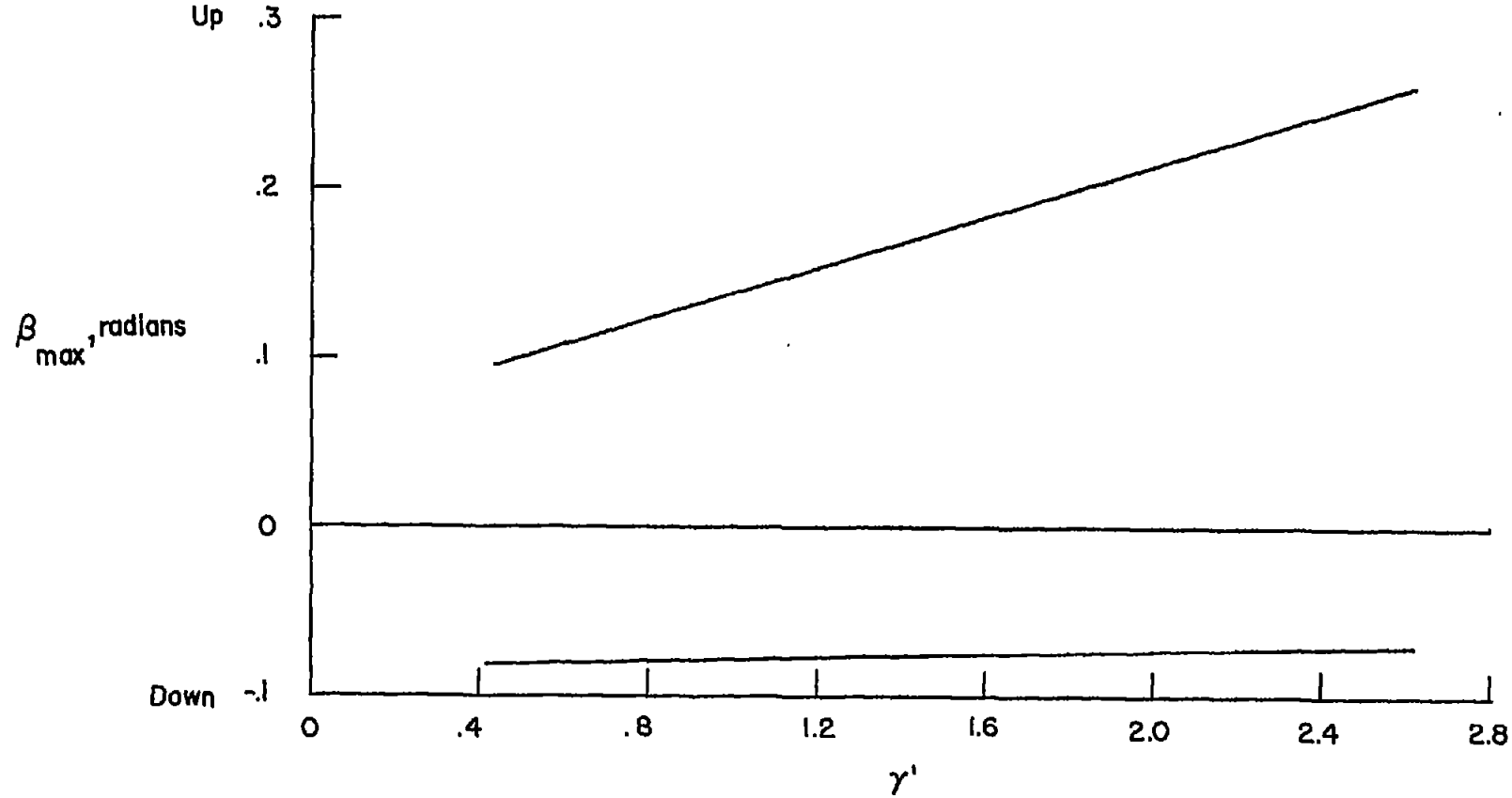

Figure 4.- Maximum steady-state amplitudes from figure 3.

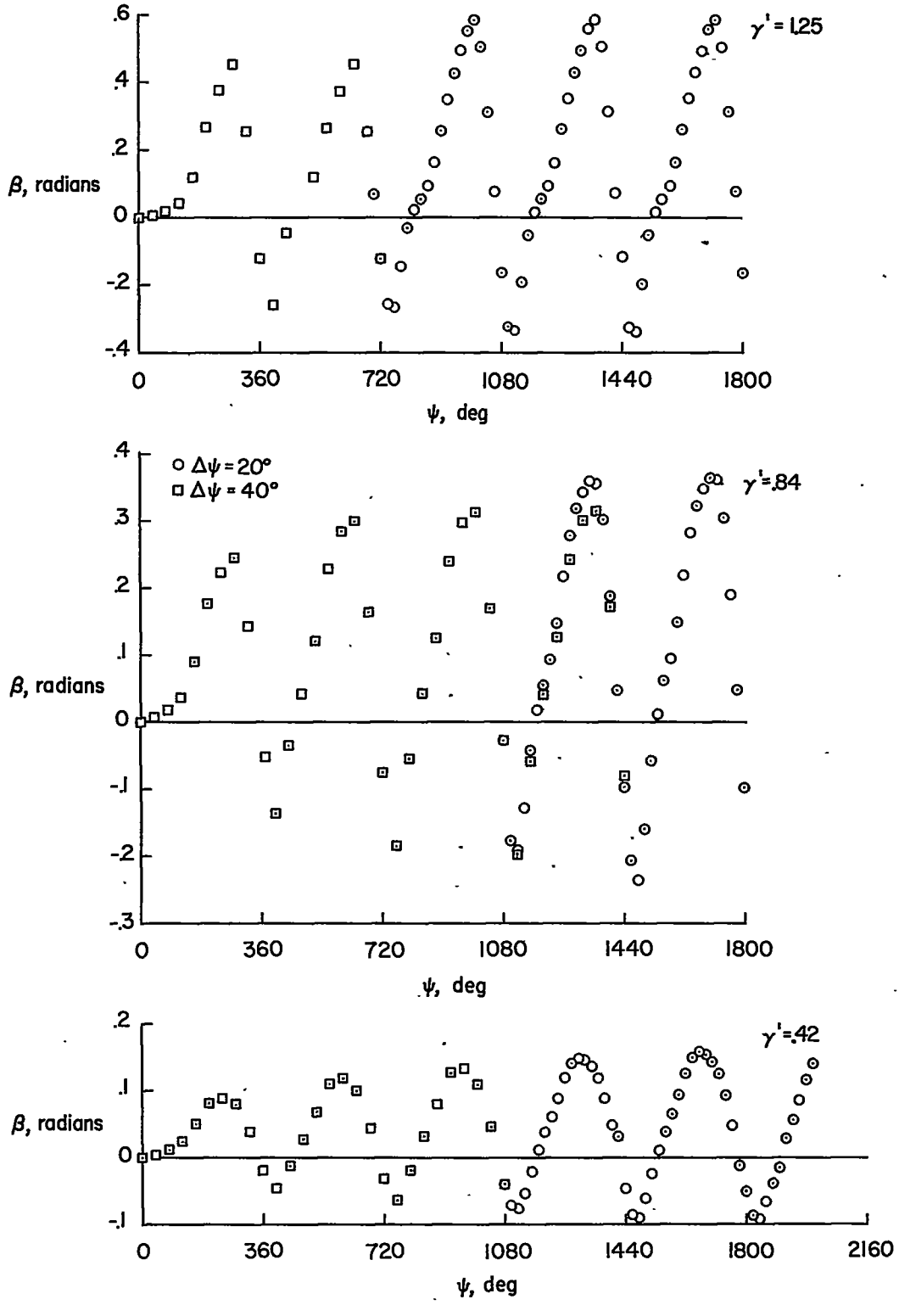

Figure 5.- Calculation of transient blade-flapping motion of free-to-cone rotor at $\mu_s = 2.2$, $\theta_{.75} = 0^\circ$, $\theta_1 = 0^\circ$, and $\lambda_s = 0.029$.

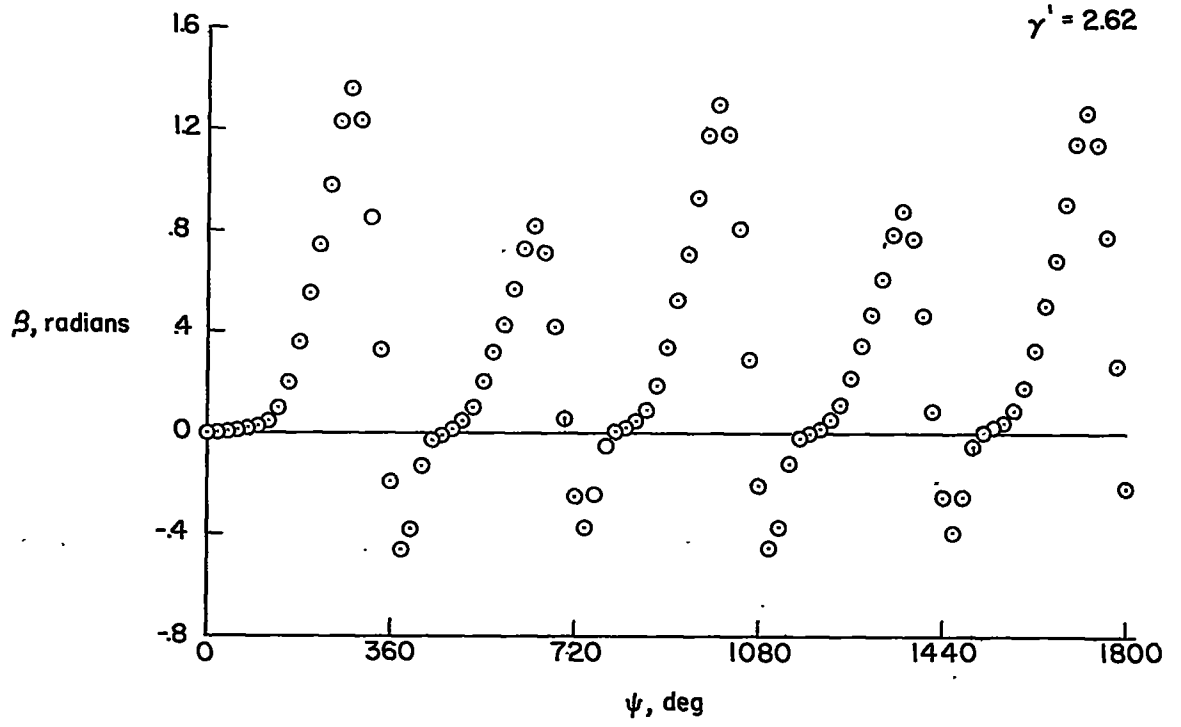

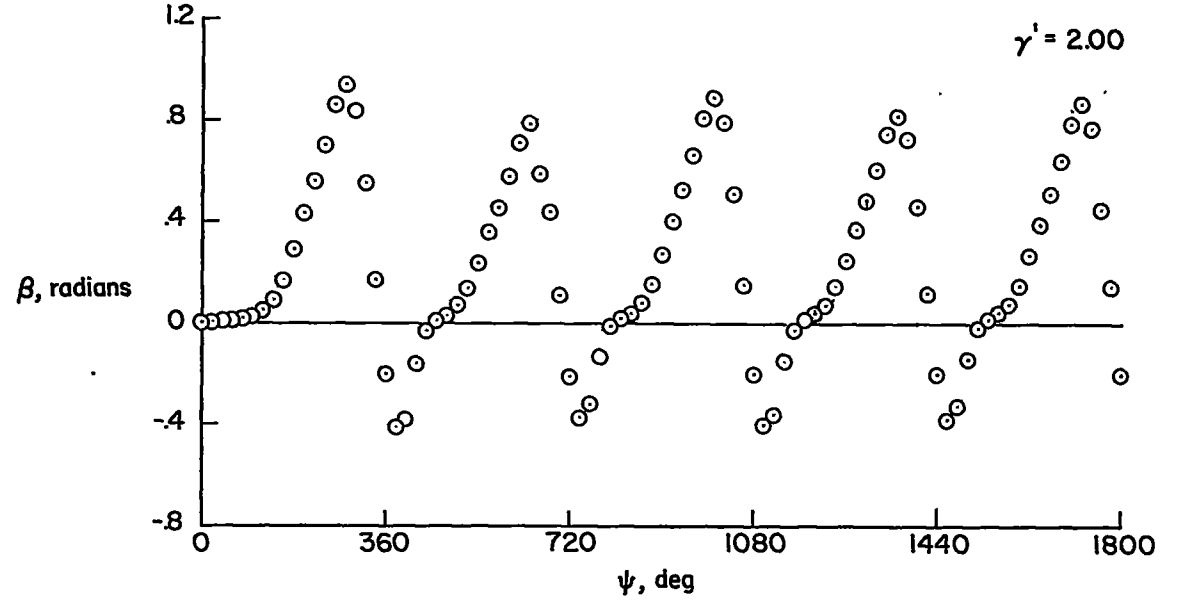

Figure 5.- Concluded.

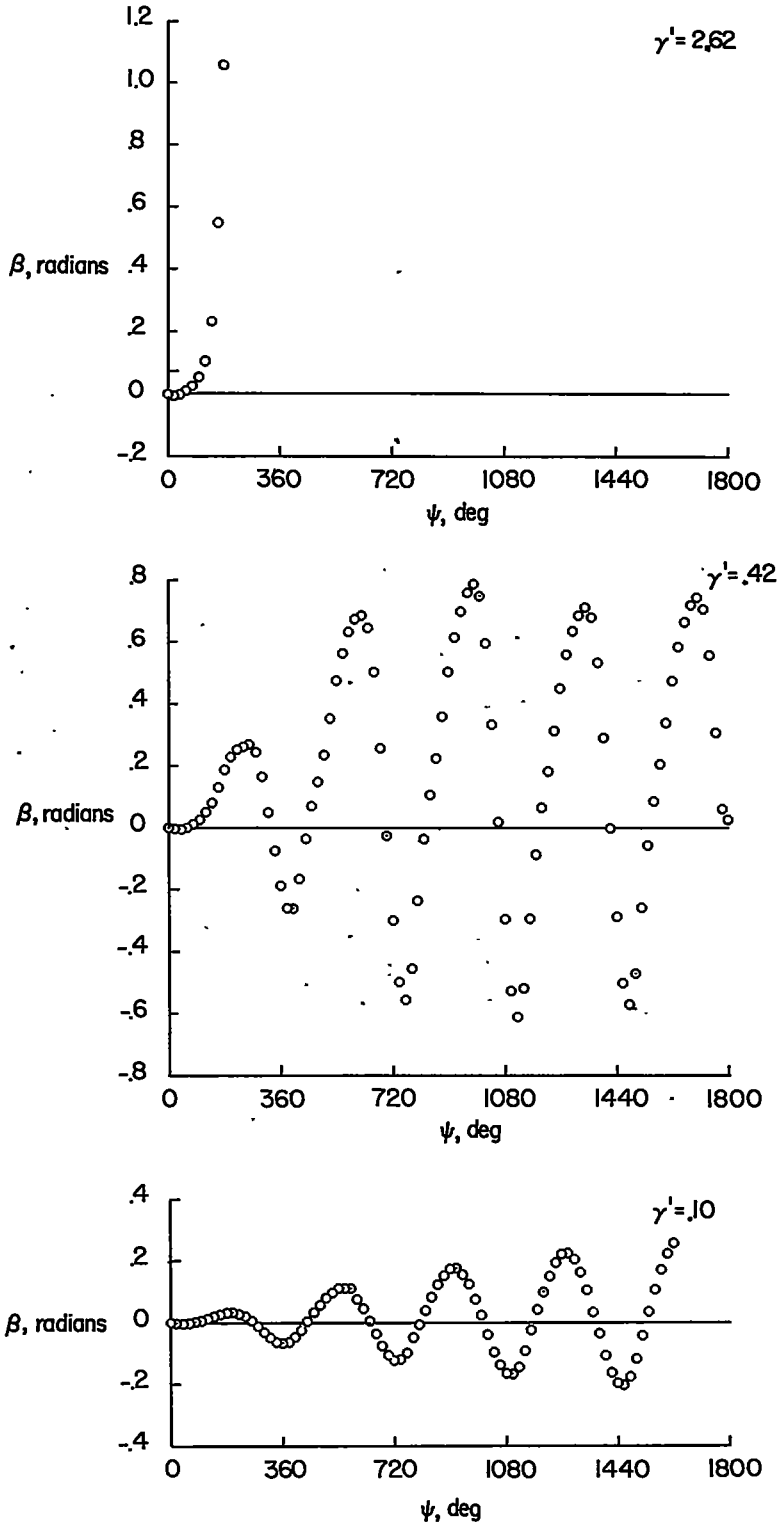

Figure 6.- Calculation of transient blade-flapping motion of free-to-cone rotor at $\mu_s = 3.0$, $\theta_{.75} = 2^\circ$, $\theta_1 = 0^\circ$, and $\lambda_s = -0.0636$.

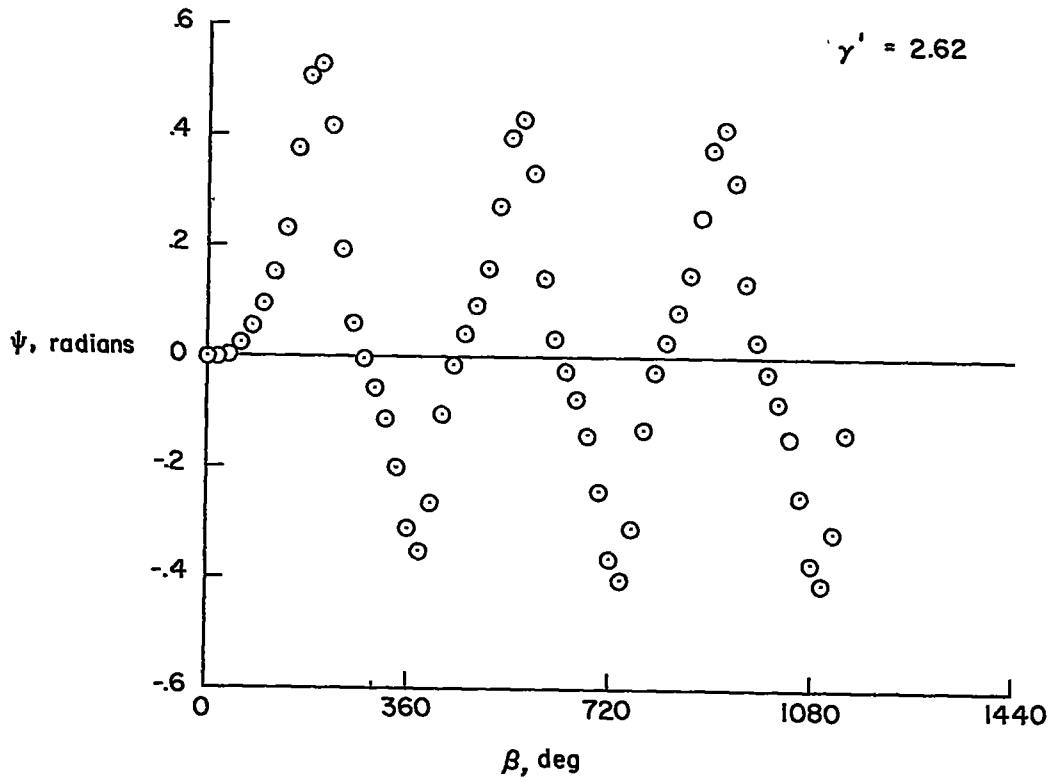

(a) $\mu_s = 3.0$; $\theta_{.75} = 2^\circ$; $\theta_1 = 0^\circ$; $\lambda_s = -0.0636$.

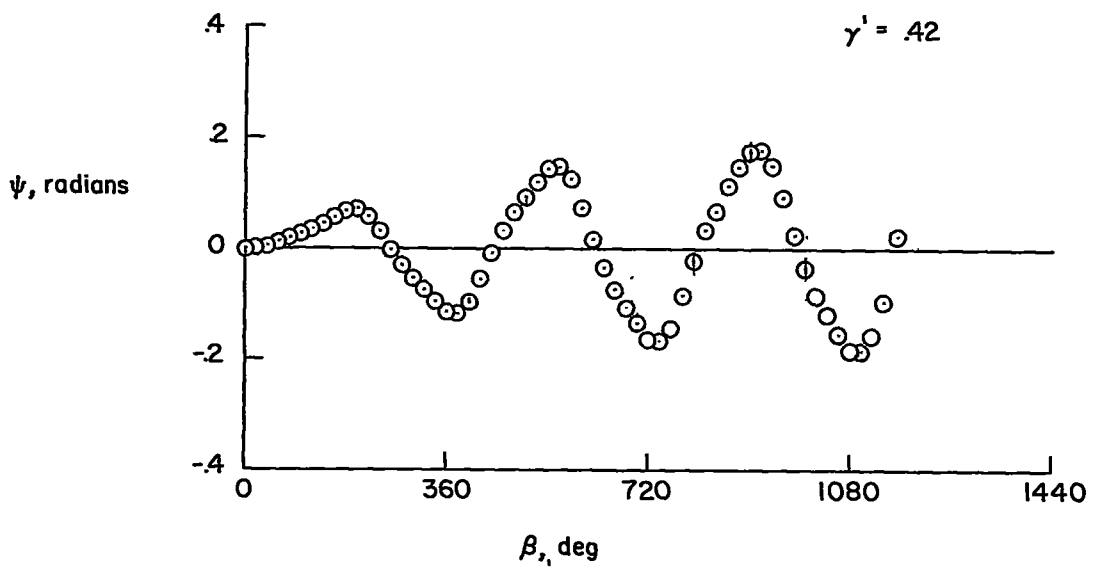

(b) $\mu_s = 2.5$; $\theta_{.75} = 0^\circ$; $\theta_1 = 0^\circ$; $\lambda_s = 0.093$.

Figure 7.- Calculation of transient blade-flapping motion of seesaw rotors.

NACA-Langley - 1-17-55 - 1000

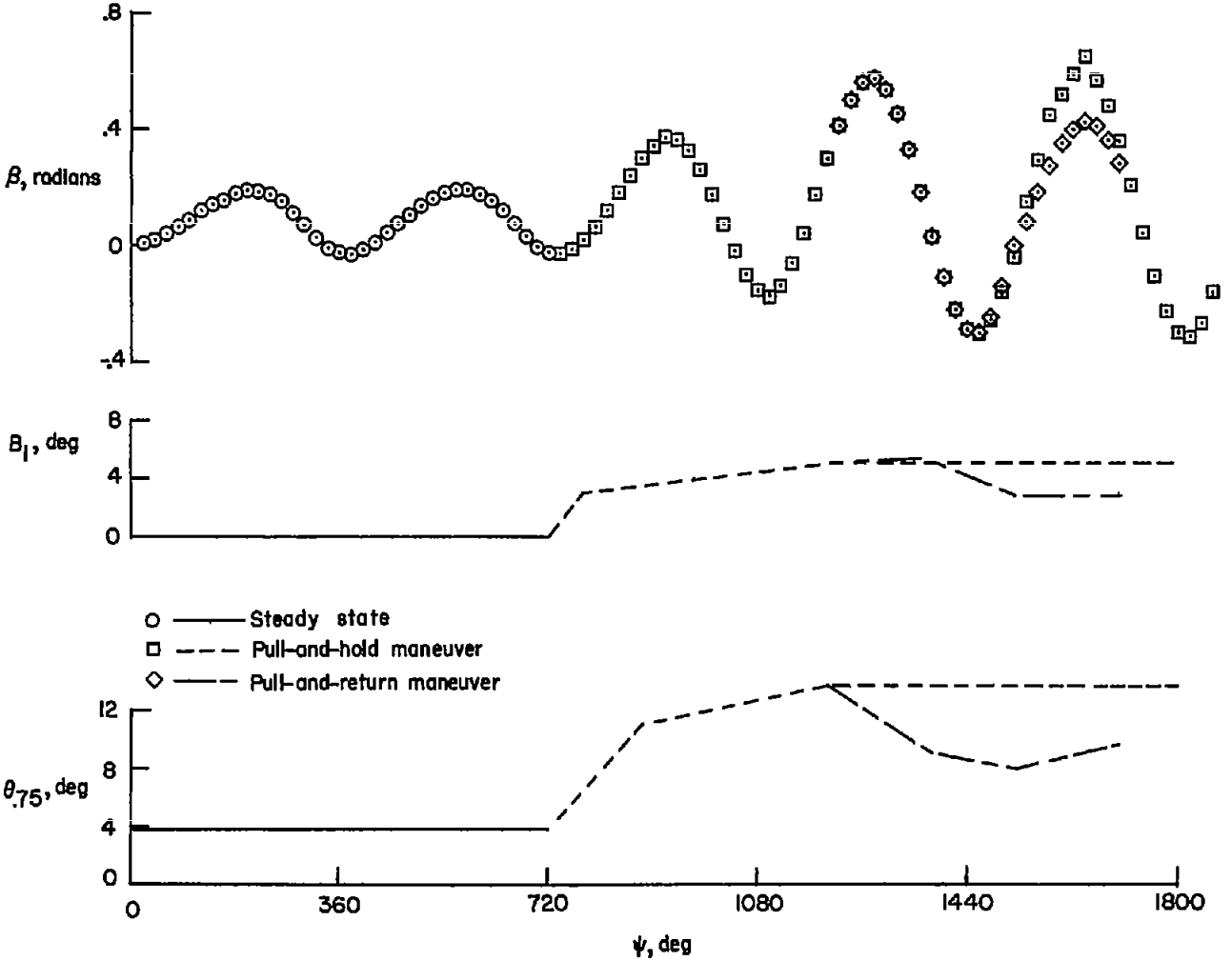

Figure 8.- Effect of control motion on blade response for free-to-cone rotor under stalled conditions. $\mu_s = 0.3$; $\theta_{.75} = 3.9^\circ$; $\theta_1 = -7^\circ$; $\lambda_s = 0.03$; $\gamma' = 1.43$.